Diffusive Mobile MC for Controlled-Release Drug Delivery with Absorbing Receiver

Trang Ngoc Cao*, Arman Ahmadzadeh‡, Vahid Jamali‡, Wayan Wicke‡,
Phee Lep Yeoh†, Jamie Evans*, and Robert Schober‡

*Department of Electrical and Electronic Engineering, The University of Melbourne, Australia
†School of Electrical and Information Engineering, The University of Sydney, Australia
‡Institute for Digital Communications, Friedrich-Alexander-University Erlangen-Nurnberg (FAU), Germany

Abstract—Nanoparticle drug carriers play an important role in facilitating efficient targeted drug delivery, i.e., improving treatment success and reducing drug costs and side effects. However, the mobility of nanoparticle drug carriers poses a challenge in designing drug delivery systems. Moreover, healing results critically depend on the rate and time duration of drug absorption. Therefore, in this paper, we aim to design a controlled-release drug delivery system with a mobile drug carrier that minimizes the total amount of released drugs while ensuring a desired rate of drug absorption during a prescribed time period. We model the mobile drug carrier as a mobile transmitter, the targeted diseased cells as an absorbing receiver, and the channel between the transceivers as a time-variant channel since the carrier mobility results in a time-variant absorption rate of the drug molecules. Based on this, we develop a molecular communication (MC) framework to design the controlled-release drug delivery system. In particular, we develop new analytical expressions for the mean, variance, probability density function, and cumulative distribution function of the channel impulse response (CIR). Equipped with the statistical analysis of the CIR, we design and evaluate the performance of the controlled-release drug delivery system. Numerical results show significant savings in the amount of released drugs compared to a constant-release rate design and reveal the necessity of accounting for drug carrier mobility for reliable drug delivery.

I. INTRODUCTION

In drug delivery systems, drug molecules are carried to the diseased cell site by nanoparticle carriers, so that the drug is efficiently delivered to the targeted site and does not affect healthy cells [1]. Experimental and theoretical studies have indicated that not only the total drug dosage but also the rate and time period of drug absorption by the diseased cell receptors are critical factors in the healing process [2], [3]. Therefore, it is important to design drug delivery systems with controlled release to minimize the total amount of released drugs while achieving a desired rate of drug absorption at the diseased site during a prescribed time period.

To this end, the mobility of drug carriers has to be accurately modeled due to the fact that after being injected or extravasated from the cardiovascular system into the tissue surrounding a targeted diseased cell site, the drug carriers may not be anchored at the targeted site but may move, mostly via diffusion [2], [4]–[6]. The diffusion of the drug carriers results in a time-variant absorption rate of drugs even if the drug release rate is constant.

The challenge of designing a controlled-release drug delivery system has been tackled from two perspectives, namely mathematical modeling [7] and experiments in vitro and vivo

[8]. In particular, the mathematical approach helps explain the experimental observations and can guide the experiments. Recently, researchers have started to design drug delivery systems based on the molecular communications (MC) paradigm where drug carriers are modeled as transmitters, diseased cells are modeled as receivers, and drug absorption is modeled as a random channel [9]. Controlled-release designs based on an MC framework were proposed in [10]–[13]. However, in these works, the transceivers were fixed and only the movement of drug particles was considered. In contrast, in this paper, we account for the mobility of the transmitter and analyze the resulting time-variant MC channel to optimize the controlled-release design. We note that time-variant MC channels with mobile transceivers were also considered in [14]–[16]. In [14], a theory for stochastic time-variant channels in mobile diffusive MC systems was developed. However, a passive receiver model was used in [14], which may not be suitable for modeling drug delivery systems since the effect of drug absorption cannot be captured. A diffusive absorbing receiver and the average distribution of the first hitting time, i.e., the mean of the channel impulse response (CIR), were derived for a one-dimensional environment without drift in [15] and with drift in [16]. Clearly, none of these works provides a complete statistical analysis of the three-dimensional (3D) time-variant channel with an absorbing receiver nor do they consider drug delivery systems.

In this paper, we analyze the 3D time-variant channel with diffusive mobile transmitter and absorbing receiver for a controlled-release drug delivery system. The main contributions are as follows:

- We design a controlled-release profile that minimizes the amount of released drugs while ensuring that the absorption rate at the diseased cells does not fall below a prescribed threshold for a given period of time. Our proposed design requires a significantly lower amount of released drugs compared to a design with constant-release rate.
- We derive the first-order (mean) and second-order (variance) moments of the time-variant CIR and exploit them for the design of the controlled-release profile.
- We derive the probability density function (PDF) and the cumulative distribution function (CDF) of the time-variant CIR for evaluation of the system performance.
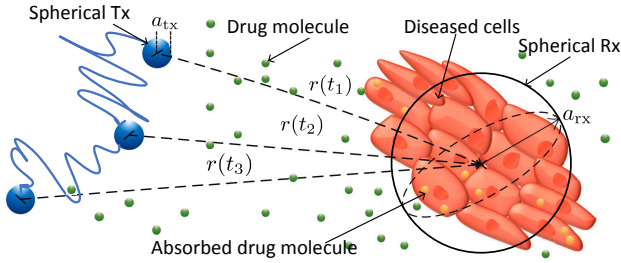- The performance of the controlled-release system is eval-

Fig. 1. System model of controlled-release drug delivery with a diffusive transmitter (Tx) and an absorbing receiver (Rx).

uated in terms of the probability that the absorption rate exceeds a targeted threshold. Our results reveal that considering transmitter mobility is crucial for meeting the system requirements.

We note that whilst this paper focuses on drug delivery, the derived analytical results for the mean, variance, PDF, and CDF of the time-variant CIR are expected to be also useful for other MC applications.

The remainder of this paper is organized as follows. In Section II, we introduce the system model. In Section III, we design the controlled-release profile for a drug delivery system based on the mean and the variance of the time-variant CIR. In Section IV, we evaluate the performance of the controlled-release drug delivery system in terms of the probability that the absorption rate exceeds a target threshold. Numerical results are presented in Section V and Section VI concludes the paper.

II. SYSTEM AND CHANNEL MODEL

In this section, we introduce the diffusive mobile MC system model and define the time-variant CIR of the absorbing receiver.

A. System Model

We apply an MC design framework to model, analyze, and optimize a controlled-release drug delivery system, see Fig. 1. The drug delivery system comprises a drug carrier releasing drug molecules and diseased cells absorbing them. We model the system environment as an unbounded 3D diffusion environment with constant temperature and viscosity. The drug carriers in drug delivery systems are typically nanoparticles, such as spherical polymers or polymer chains, having a size not smaller than $100\,\mathrm{nm}$ [5]. Hence, we model the drug carrier as a spherical transmitter, denoted by Tx, with radius a_{tx}. Furthermore, we model the Tx as transparent, i.e., it does not have any effect on the receiver or drug molecules after they are released from its center. This model is valid since in reality the drug carrier is designed to carry drug molecules and interaction with the drug or the receiver is not intended. The drug carriers can be directly injected or extravasated from the blood to the interstitial tissue near the diseased cells (e.g. a tumor), where they start to move. The movement of the drug carrying nanoparticles in the tissue is caused by diffusion and convection mechanisms but diffusion is expected to be dominant in most cases [2], [4]–[6]. At the tumor site, the drug carrier releases drug molecules of type X, which also

diffuse in the tissue [2]. Hence, we adopt Brownian motion to model the diffusion of the Tx and the molecules X [1]. When the drug molecules hit the tumor, they are absorbed by receptors on the surface of the diseased cells [2], [3]. For convenience, we model the tumor as a spherical absorbing receiver, denoted by Rx. In reality, the colony of cancer cells may potentially have a different geometry, of course. However, as an abstract approximation, we model the cancer cells as one effective spherical receiver with radius a_{rx} and with a surface area equivalent to the total surface area of the tumor, i.e., the absorption on both the actual and the modeled surfaces is expected to be comparable [4].

The absorption rate ultimately determines the therapeutic impact of the drug [2], [3]. Thus, we make achieving a desired absorption rate the objective for the system design. We will formally define the absorption rate in the next subsection but before doing so, we define the parameters and assumptions used in the system model. We assume that the diffusion of the Tx and molecules X is independent of each other with corresponding diffusion coefficients, D_{Tx} and D_{X}, respectively. We denote the time-varying distance between the centers of the Tx and the Rx at time t by $r(t)$. In a 3D Cartesian space, $r(t)$ can be represented as $r(t) = (r_x, r_y, r_z)$. Then, the distance between the centers of the transceivers at time zero is denoted by $r(t = 0) = r_0 = (r_{x0}, r_{y0}, r_{z0})$. We assume that the Tx can release molecules during a period of time denoted by T_{Tx}. After this period, the drug carrier may be removed by blood circulation or run out of drugs. We assume that the Tx releases molecules at its center instantaneously and discretely over time. Let t_i and Δt_i denote the time instant of the i-th release and the duration of the interval between the i-th and the $(i + 1)$-th release, respectively. We have $i \in \{1, \ldots, I\}$, where I is the total number of releases during T_{Tx}. We note that a continuous release can be approximated by letting $\Delta t_i \to 0$, i.e., $I \to \infty$. Furthermore, let α_i and $A = \sum_{i=1}^{I} \alpha_i$ denote the number of drug molecules released at time t_i and the total amount of drugs released during T_{Tx}, respectively.

B. Impulse Response of the Diffusive Channel

To evaluate the drug absorption rate at the Rx given the drug release profile at the Tx, we first need to derive the CIR. Let $h(t, \tau)$ denote the hitting rate, i.e., the absorption rate of a given molecule, τ [s] after its release at time t at the center of Tx. Note that the distance between the centers of the Tx and the Rx, i.e., $r(t)$, is a random variable and a function of t. Hence, $h(t, \tau)$ may be referred to as the CIR, which completely characterizes the time-variant channel. In $h(t, \tau)$, variable t denotes the time instant of the release of the molecules at Tx while variable τ represents the time period between the release at the Tx and the absorption at the Rx.

For a given $r(t)$, the CIR $h(t, \tau)$ is given by [17]

$$h(t, \tau) = \frac{a_{\mathrm{rx}}}{\sqrt{4\pi D_{\mathrm{X}} \tau^3}} \left(1 - \frac{a_{\mathrm{rx}}}{r(t)}\right) \exp\left(-\frac{(r(t) - a_{\mathrm{rx}})^2}{4 D_{\mathrm{X}} \tau}\right),$$

(1)

for $\tau > 0$, and $h(t, \tau) = 0$, for $\tau \leqslant 0$. From the definition of $h(t, \tau)$, for $\Delta\tau \to 0$, we can interpret $h(t, \tau)\Delta\tau$ as the

probability of absorption of a molecule by the Rx between times τ and $\tau + \Delta\tau$ after the release at time t. If α_i molecules are released at the Tx at time t_i, the expected number of molecules absorbed at the Rx between times t and $t + \Delta t$, for $\Delta t \to 0$, is equal to $\alpha_i h(t_i, t - t_i)\Delta t$, for $\tau = t - t_i$. During the period $[0, t]$, a total amount of $A_t = \sum_i \alpha_i, \forall i | t_i < t$, of drugs are released and thus, an expected total amount of $y(t) = \sum_i \alpha_i h(t_i, t - t_i)\Delta t, \forall i | t_i < t$, of drugs are absorbed between times t and $t + \Delta t$, for $\Delta t \to 0$. Let $g(t)$ denote the absorption rate of molecules X at the Rx at time t, i.e., $g(t) = y(t)/\Delta t, \Delta t \to 0$. Then, we have

$$g(t) = \sum_{\forall i | t_i < t} \alpha_i h(t_i, t - t_i). \tag{2}$$

As mentioned before, the absorption rate $g(t)$ at the tumor directly affects the healing efficacy of the drug. Hence, we will design the drug delivery system such that $g(t)$ does not fall below a prescribed value.

III. CONTROLLED-RELEASE DESIGN

We first formulate the controlled-release design problem and then derive the mean and variance of the stochastic time-variant channel to solve the problem.

A. Problem Formulation

The treatment of many diseases requires the diseased cells to absorb a minimum rate of drugs during a given period of time [3]. To design an efficient drug delivery system satisfying this requirement, we optimize the amounts of released drugs α_i such that the total amount of released drugs, $A = \sum_{i=1}^I \alpha_i$, is minimized and the absorption rate $g(t)$ is equal to or larger than a targeted rate, $\theta(t)$, for a period of time, denoted by T_{Rx}. Depending on the properties of the tumor, $\theta(t)$ may vary with time. Since $g(t)$ is a random variable, we will design the system based on the first and second order moments of the CIR. In particular, we minimize $A = \sum_{i=1}^I \alpha_i$ subject to the constraint that the mean of $g(t)$ minus a certain deviation is equal to or above a threshold during T_{Rx}, i.e., $\text{E}\{g(t)\} - \beta\Gamma\{g(t)\} \geqslant \theta(t)$ for $0 \leqslant t \leqslant T_{\text{Rx}}$, where $\text{E}\{\cdot\}$ and $\Gamma\{\cdot\}$ denote expectation and standard deviation, respectively, and β is a coefficient determining how much deviation from the mean is taken into account. Based on (2), the constraint can be written as a function of α_i as follows

$$\text{E}\{g(t)\} - \beta\Gamma\{g(t)\} \overset{(a)}{\geqslant} \tag{3}$$
$$\sum_{\forall i | t_i < t} \alpha_i \left(\text{E}\{h(t_i, t - t_i)\} - \beta\Gamma\{h(t_i, t - t_i)\} \right) \geqslant \theta(t),$$

where $0 \leqslant t \leqslant T_{\text{Rx}}$. Inequality (a) in (3) is due to Minkowski's inequality [18]. Note that we may not be able to find α_i such that (3) holds for all values of β and $\theta(t)$. However, when $\text{E}\{h(t_i, t - t_i)\} > \beta\Gamma\{h(t_i, t - t_i)\}$, i.e., either β or $\Gamma\{h(t_i, t - t_i)\}$ is small, so that $\beta\Gamma\{h(t_i, t - t_i)\}$ is sufficiently small, we can always find α_i so that (3) holds for arbitrary $\theta(t)$. Since time t is a continuous variable, the constraint in (3) has to be satisfied for all values of t, $0 \leqslant t \leqslant T_{\text{Rx}}$, and thus there is an infinite number of constraints, each of which corresponds to one value of t. Therefore, we simplify

the problem by relaxing the constraints to hold only for a finite number of time instants $t = t_n = n\Delta t_n$, where $n = 1, \ldots, N$ and $\Delta t_n = T_{\text{Rx}}/N$. Then, the optimization problem for the design of α_i can be formulated as

$$\min_{\alpha_i \geqslant 0, \forall i} A = \sum_{i=1}^I \alpha_i \tag{4a}$$
$$\text{s.t.} \sum_{i, t_i < t} \alpha_i \left(m(t_i, n\Delta t_n - t_i) - \beta\sigma(t_i, n\Delta t_n - t_i) \right)$$
$$\geqslant \theta(n\Delta t_n - t_i), \text{ for } n = 1, \ldots, N, \tag{4b}$$

where $m(t, \tau)$ and $\sigma(t, \tau)$ are the mean and the standard deviation of $h(t, \tau)$, respectively. In order to solve (4), we need to derive analytical expressions for $m(t, \tau)$ and $\sigma(t, \tau)$. Moreover, since $h(t, \tau)$ is a function of $r(t)$, which is a random variable, we first need to derive the distribution of $r(t)$ before deriving $m(t, \tau)$ and $\sigma(t, \tau)$. Having $m(t, \tau)$ and $\sigma(t, \tau)$ and treating the α_i as real numbers, (4) can be readily solved as a linear program using existing algorithms or numerical software such as MATLAB. We note that although the numbers of molecules α_i are integers, for tractability, we solve (4) for real α_i and quantize the results to the nearest integer values.

Note that the problem in (4) is statistical in nature and provides instructive guidance for the offline design of the system.

B. Distribution of the Tx-Rx Distance in a Diffusive System

In this subsection, we derive the distribution of $r(t)$. If the diffusion of Tx follows Brownian motion in the entire 3D environment, we have $r_x \sim \mathcal{N}(r_{x0}, 2D_{\text{Tx}}t), r_y \sim \mathcal{N}(r_{y0}, 2D_{\text{Tx}}t), r_z \sim \mathcal{N}(r_{z0}, 2D_{\text{Tx}}t)$. Then, $\frac{r(t)}{\sqrt{2D_{\text{Tx}}t}}$, denoted by γ, follows a noncentral chi distribution, denoted by $\mathcal{X}_k(\lambda)$, [19]

$$\gamma = \frac{r(t)}{\sqrt{2D_{\text{Tx}}t}} = \sqrt{\frac{r_x^2 + r_y^2 + r_z^2}{2D_{\text{Tx}}t}} \sim \mathcal{X}_k(\lambda), \tag{5}$$

with parameters $k = 3$ and $\lambda = \sqrt{\frac{r_{x0}^2 + r_{y0}^2 + r_{z0}^2}{2D_{\text{Tx}}t}} = \frac{r_0}{\sqrt{2D_{\text{Tx}}t}}$. Thus, we can obtain the PDF of r as follows

$$f_{r(t)}(r) \overset{(a)}{=} \frac{1}{\sqrt{2D_{\text{Tx}}t}} f_\gamma(\gamma) \tag{6}$$
$$\overset{(b)}{=} \frac{r}{r_0\sqrt{\pi D_{\text{Tx}}t}} \exp\left(-\frac{r^2 + r_0^2}{4D_{\text{Tx}}t}\right) \sinh\left(\frac{r_0 r}{2D_{\text{Tx}}t}\right),$$

where $f_\gamma(\gamma)$ is the PDF of γ. Equality (a) in (6) exploits the fact that γ is a function of $r(t)$ [20, Eq. 5-16]. Equality (b) in (6) is obtained from the expression of the PDF $f_\gamma(\gamma)$ [19].

Remark 1: Note that (6) was derived under the assumption that the Tx can diffuse in the entire 3D environment. In reality, the Tx cannot be inside the Rx, i.e., it does not interact with the Rx, and thus will be reflected when it hits the Rx boundary. Hence, the actual $f_{r(t)}(r)$ may differ from (6), e.g. $f_{r(t)}(r) = 0$ for $r < a_{\text{tx}} + a_{\text{rx}}$. However, we note that for very small r, i.e., $r \approx 0$, (6) does approach zero. Hence, (6) is a valid approximation for the actual $f_{r(t)}(r)$. The validity of this approximation is evaluated in Section V via simulations.

C. Statistical Moments of Diffusive Channel

In this subsection, we derive the statistical moments of the diffusive channel, i.e., $m(t,\tau)$ and $\sigma^2(t,\tau)$. In particular, $m(t,\tau)$ is obtained as

$$m(t,\tau) = \int_0^\infty h(t,\tau)\big|_{r(t)=r}\, f_{r(t)}(r)\mathrm{d}r. \tag{7}$$

A closed-form expression of (7) is provided in the following theorem.

Theorem 1: The mean of the impulse response of a time-variant MC channel with diffusive molecules transmitted by a diffusive transparent transmitter and absorbed by an absorbing receiver is given by

$$m(t,\tau) = \frac{a_{\mathrm{rx}}}{4\sqrt{\pi}\,(D_{\mathrm{X}}\tau + D_{\mathrm{Tx}}t)r_0\tau} \exp\left(-\frac{a_{\mathrm{rx}}^2}{4D_{\mathrm{X}}\tau} - \frac{r_0^2}{4D_{\mathrm{Tx}}t}\right)$$
$$\times \left(-e^{\frac{b(t,\tau)^2}{4a(t,\tau)}}\left(\frac{b(t,\tau)}{2a(t,\tau)} + a_{\mathrm{rx}}\right)\mathrm{erfc}\left(\frac{b(t,\tau)}{2\sqrt{a(t,\tau)}}\right)\right.$$
$$\left. + e^{\frac{c(t,\tau)^2}{4a(t,\tau)}}\left(\frac{c(t,\tau)}{2a(t,\tau)} + a_{\mathrm{rx}}\right)\mathrm{erfc}\left(\frac{c(t,\tau)}{2\sqrt{a(t,\tau)}}\right)\right), \tag{8}$$

where $\mathrm{erfc}(\cdot)$ is the complementary error function and for compactness, $a(t,\tau)$, $b(t,\tau)$, and $c(t,\tau)$ are defined as follows

$$a(t,\tau) = \frac{1}{4D_{\mathrm{X}}\tau} + \frac{1}{4D_{\mathrm{Tx}}t}, \qquad b(t,\tau) = -\frac{a_{\mathrm{rx}}}{2D_{\mathrm{X}}\tau} - \frac{r_0}{2D_{\mathrm{Tx}}t},$$
$$c(t,\tau) = -\frac{a_{\mathrm{rx}}}{2D_{\mathrm{X}}\tau} + \frac{r_0}{2D_{\mathrm{Tx}}t}. \tag{9}$$

Proof: Substituting (1) and (6) into (7) and using the integrals given by [21, Eq. (2.3.15.4) and Eq. (2.3.15.7)], we obtain the expression for $m(t,\tau)$ in (8). □

Remark 2: We note that $m(t,\tau)$ approaches zero when $t \to \infty$ since $r(t)$ increases on average due to diffusion.

Next, we obtain the variance of $h(t,\tau)$ as

$$\sigma^2(t) = \phi(t) - m^2(t), \tag{10}$$

where $\phi(t) = \mathrm{E}\left\{h^2(t,\tau)\right\}$. The following lemma gives an analytical expression for $\phi(t)$.

Lemma 1: For the considered channel, $\phi(t)$ is given by

$$\phi(t) = \hat{k}(t)\int_0^\infty \left[\exp\left(-\hat{a}(t)r^2 - \hat{b}(t)r\right)\right. \tag{11}$$
$$\left. - \exp\left(-\hat{a}(t)r^2 - \hat{c}(t)r\right)\right]\left(r - 2a_{\mathrm{rx}} + \frac{a_{\mathrm{rx}}^2}{r}\right)\mathrm{d}r,$$

where

$$\hat{k}(t) = \frac{a_{\mathrm{rx}}^2 e^{-\frac{a_{\mathrm{rx}}^2}{2D_{\mathrm{X}}\tau} - \frac{r_0^2}{4D_{\mathrm{Tx}}t}}}{8D_{\mathrm{X}}\pi\tau^3 r_0\sqrt{\pi D_{\mathrm{Tx}}t}}, \qquad \hat{a}(t) = \frac{1}{2D_{\mathrm{X}}\tau} + \frac{1}{4D_{\mathrm{Tx}}t},$$
$$\hat{b}(t) = -\frac{a_{\mathrm{rx}}}{D_{\mathrm{X}}\tau} - \frac{r_0}{2D_{\mathrm{Tx}}t}, \qquad \hat{c}(t) = -\frac{a_{\mathrm{rx}}}{D_{\mathrm{X}}\tau} + \frac{r_0}{2D_{\mathrm{Tx}}t}. \tag{12}$$

Proof: Substituting (1) and (6) into the definition of $\phi(t)$ and simplifying the expression, we obtain (11). □

Remark 3: The expression in (11) comprises integrals of the form $\int_0^\infty \exp\left(ax^2 + bx\right)/x\,\mathrm{d}x$, where a and b are constants, and cannot be obtained in closed form. However, these integrals can be evaluated numerically in a straight forward manner.

IV. PERFORMANCE ANALYSIS

Since $g(t)$ is random, we cannot always guarantee $g(t) \geqslant \theta(t)$. Moreover, since $g(t) \geqslant \theta(t)$ is required for proper operation of the system, we evaluate the system performance in terms of the probability that $g(t) \geqslant \theta(t)$, denoted by $P_\theta = \Pr\{g(t) \geqslant \theta(t)\}$. In this section, we first present a theoretical framework for evaluation of the system performance in terms of P_θ expressed as a function of the PDF and CDF of the CIR, before finally deriving the PDF and CDF of the CIR.

A. System Performance

The probability P_θ is given in the following theorem.

Theorem 2: The system performance metric P_θ can be expressed as

$$P_\theta = 1 - f_{\alpha_1 h(t-t_1,t_1)}\left(\theta(t)\right) * \cdots * f_{\alpha_{\breve{i}-1}h\left(t-t_{\breve{i}-1},t_{\breve{i}-1}\right)}\left(\theta(t)\right)$$
$$* F_{\alpha_{\breve{i}}h(t-t_{\breve{i}},t_{\breve{i}})}\left(\theta(t)\right), \tag{13}$$

where $*$ denotes convolution, $\breve{i} = 1,2,\ldots$ satisfies $t_{\breve{i}} \leqslant t$, and $f_{\{\cdot\}}$ and $F_{\{\cdot\}}$ denote the PDF and CDF of the random variable in the subscript, respectively. In (13), we define $f_{\alpha_{\breve{i}}h(t-t_{\breve{i}},t_{\breve{i}})}\left(\theta(t)\right) = 1/\alpha_{\breve{i}} \times f_{h(t-t_{\breve{i}},t_{\breve{i}})}\left(\theta(t)/\alpha_{\breve{i}}\right)$ and $F_{\alpha_{\breve{i}}h(t-t_{\breve{i}},t_{\breve{i}})}\left(\theta(t)\right) = F_{h(t-t_{\breve{i}},t_{\breve{i}})}\left(\theta(t)/\alpha_{\breve{i}}\right)$.

Proof: From the definition of the CDF, we have

$$P_\theta = 1 - F_{g(t)}\{\theta(t)\} = 1 - \int_0^{\theta(t)} f_{g(t)}(g)\mathrm{d}g. \tag{14}$$

Due to the summation of independent random variables in (2), i.e., independent releases at t_i, we have

$$f_{g(t)}(g) = \left(f_{\alpha_1 h(t-t_1,t_1)} * \cdots * f_{\alpha_{\breve{i}}h(t-t_{\breve{i}},t_{\breve{i}})}\right)(g). \tag{15}$$

Substituting (15) into (14), and using the integration property of the convolution, i.e.,

$$\int_0^{\theta(t)}\left(f_{\alpha_1 h(t-t_1,t_1)} * \cdots * f_{\alpha_{\breve{i}}h(t-t_{\breve{i}},t_{\breve{i}})}\right)(g)\mathrm{d}g \tag{16}$$
$$= f_{\alpha_1 h(t-t_1,t_1)}\left(\theta(t)\right) * \cdots * \int_0^{\theta(t)} f_{\alpha_{\breve{i}}h(t-t_{\breve{i}},t_{\breve{i}})}(g)\mathrm{d}g,$$

and using the definition of the CDF, we obtain (13). □
According to (13), P_θ can be evaluated based on exact expressions for the PDF and the CDF of $h(t,\tau)$, which will be derived in the next subsection.

Furthermore, we note that a minimum value of P_θ can be guaranteed based on statistical moments of the CIR, without knowledge of the PDF and the CDF, as shown in the following proposition.

Proposition 1: A lower bound on $P_\theta = \Pr\{g(t) \geqslant \theta(t)\}$ is given as follows

$$P_\theta \geqslant 1 - \frac{1}{\beta^2}. \tag{17}$$

Proof: By using (3) and the Chebyshev inequality [20], we obtain

$$P_\theta \overset{(a)}{\geqslant} \Pr\left\{|g(t) - \mathrm{E}\{g(t)\}| \leqslant \mathrm{E}\{g(t)\} - \theta(t)\right\} \tag{18}$$
$$\overset{(b)}{\geqslant} 1 - \frac{\Gamma^2\{g(t)\}}{(\mathrm{E}\{g(t)\} - \theta(t))^2} \overset{(c)}{\geqslant} 1 - \frac{1}{\beta^2},$$

where (a) can be obtained easily by expanding the absolute value on the right-hand side, (b) is due to the Chebyshev inequality, and (c) is due to (3). This completes the proof. □

Remark 4: Proposition 1 is not only useful for evaluating the system performance, but also provides a guideline for the design of the controlled release of drugs. For example, to ensure $P_\theta \geqslant 0.75$, from (17), we obtain $\beta = 2$. Note that a useful bound can only be obtained based on (17) when $\beta > 1$.

B. Distribution Functions of the CIR

The PDF of the CIR is given in the following theorem.

Theorem 3: The PDF of the impulse response of a time-variant channel with diffusive molecules transmitted by a diffusive transparent transmitter and absorbed by an absorbing receiver is given by

$$
\begin{cases}
f_{h(r(t),\tau)}(h) = \frac{f_{r(t)}(r_1(h))}{h'(r_1(h),\tau)} - \frac{f_{r(t)}(r_2(h))}{h'(r_2(h),\tau)}, & \text{for } 0 \leqslant h < h^\star, \\
f_{h(r(t),\tau)}(h) \rightarrow \infty, & \text{for } h = h^\star,
\end{cases}
\tag{19}
$$

where $h(r(t),\tau)$ denotes $h(t,\tau)$ as a function of $r(t)$ and τ, $f_{r(t)}(r)$ is given by (6), $r_1(h)$ and $r_2(h)$, $r_1(h) < r_2(h)$, are the solutions of the equation $h(r(t),\tau) = h$, $h^\star$ is the maximum value of $h(r(t),\tau)$ for all values of $r(t)$, and $h'(r,\tau)$ is given by

$$
h'(r,\tau) = \frac{a_{\text{rx}}}{\sqrt{4\pi D_X \tau^3}} \exp\left(-\frac{(r - a_{\text{rx}})^2}{4D_X\tau}\right)
\tag{20}
$$
$$
\times \left(\frac{a_{\text{rx}}}{r^2} - \frac{(r - a_{\text{rx}})}{2D_X\tau}\left(1 - \frac{a_{\text{rx}}}{r}\right)\right).
$$

Proof: From (20), we observe that $h'(r,\tau) = \frac{\partial h(r,\tau)}{\partial r} = 0$ is equivalent to a cubic equation in r, given by $ar^3 + br^2 + cr + d = 0$, with properly defined coefficients a, b, c, d and discriminant $\Delta = 18abcd - 4b^3d + b^2c^2 - 4ac^3 - 27a^2d^2 < 0$. Hence, $h'(r,\tau) = 0$ has only one real valued solution, denoted by $r^\star$. Then, from (20), we obtain that $h'(r_1,\tau) > 0$ for $r_1 < r^\star$, $h'(r_2,\tau) < 0$ for $r_2 > r^\star$, and $h'(r,\tau) = 0$ for $h = h^\star$, where $h^\star = h(r^\star,\tau)$ is the maximum value of $h(r,\tau)$. Finally, we derive (19) by exploiting [20, Eq. 5-16] for the PDF of functions of random variables. □

The CDF of $h(t,\tau)$ is given in the following corollary.

Corollary 1: The CDF of the impulse response of a time-variant channel with diffusive molecules transmitted by a diffusive transparent transmitter and absorbed by an absorbing receiver is given by

$$
F_{h(r(t),\tau)}(h) = F_{r(t)}(r_1(h)) + 1 - F_{r(t)}(r_2(h)),
\tag{21}
$$

for $0 \leqslant h \leqslant h^\star$, where $F_{r(t)}(r)$ is the CDF of r and is given by

$$
F_{r(t)}(r) = 1 - \mathbf{Q}_{\frac{3}{2}}\left(\lambda, \frac{r}{\sqrt{2D_{\text{Tx}}t}}\right).
\tag{22}
$$

Here, λ is defined in (5) and $\mathbf{Q}_M(a,b)$ is the Marcum Q-function as defined in [19].

Proof: From the definition of the CDF and (19), we have

$$
F_{h(r(t),\tau)}(h) = \int_0^h f_{h(r(t),\tau)}(\check{h})d\check{h}
\tag{23}
$$
$$
= \int_0^h \frac{f_{r(t)}(\check{r}_1(\check{h}))}{\partial h(\check{r}_1,\tau)/\partial \check{r}_1} - \frac{f_{r(t)}(\check{r}_2(\check{h}))}{\partial h(\check{r}_2,\tau)/\partial \check{r}_2}d\check{h}
$$
$$
= \int_0^{r_1(h)} f_{r(t)}(\check{r}_1)d\check{r}_1 - \int_\infty^{r_2(h)} f_{r(t)}(\check{r}_2)d\check{r}_2
$$
$$
= F_{r(t)}(r_1(h)) + 1 - F_{r(t)}(r_2(h)),
$$

where $\check{r}_1$ and $\check{r}_2$, $\check{r}_1 < \check{r}_2$, are the solutions of the equation $h(\check{r},\tau) = \check{h}$. Moreover, since $\frac{r(t)}{\sqrt{2D_{\text{Tx}}t}}$ follows a noncentral chi distribution, we obtain (22) as [19]

$$
F_{r(t)}(r) = F_{\frac{r(t)}{\sqrt{2D_{\text{Tx}}t}}}\left(\frac{r}{\sqrt{2D_{\text{Tx}}t}}\right) = 1 - \mathbf{Q}_{\frac{3}{2}}\left(\lambda, \frac{r}{\sqrt{2D_{\text{Tx}}t}}\right).
\tag{24}
$$

This completes the proof. □

We note that the analytical expressions for the PDF and CDF of $h(t,\tau)$ in Theorem 3 and Corollary 1, respectively, are not in closed form. Therefore, the evaluation of the system performance in (13) can be approximated by a discrete convolution which is easily evaluated numerically.

Remark 5: The results for the mean, variance, PDF, and CDF of the CIR in Sections III-C and IV-B can also be applied for applications where both the transmitter and the receiver undergo diffusion. In this case, we have to replace D_X and D_{Tx} in the derived expressions by $D_1 = D_X + D_{\text{Rx}}$ and $D_2 = D_{\text{Tx}} + D_{\text{Rx}}$, respectively. D_1 and D_2 are the effective diffusion coefficients capturing the relative movements of the molecules X and the Rx and the relative movements of the Tx and the Rx, respectively, see [14].

V. NUMERICAL RESULTS

In this section, we provide numerical results to evaluate the accuracy of the derived expressions and the efficiency of the proposed drug delivery system. In the simulations, we use a particle-based simulation of Brownian motion, where the transmitter performs a random displacement in discrete time steps of length Δt^{st} seconds. The random displacement of the transmitter in each step is modeled as a Gaussian random variable with zero mean and standard deviation $\sqrt{2D_{\text{Tx}}\Delta t^{\text{st}}}$. Furthermore, in the simulations, we also take into account the reflection of the Tx when the Tx hits the Rx. Moreover, we adopt Monte-Carlo simulation by averaging our results over a large number of independent realizations of the Tx movement.

For all numerical results, we use the set of simulation parameters in Table I, unless otherwise stated. The parameters in Table I are chosen to match real system parameters, e.g. the diffusion constants D_X of drug molecules vary from 10^{-9} to 10^{-14} m^2/s [6], the drug carriers have sizes $\geqslant 100$ nm [5], the size of tumor cells is on the order of μm, and the drug carriers can be injected or extravasated from the cardiovascular system in the tissue surrounding the targeted diseased cell site [2], i.e., close to the tumor cells. The dosing periods in drug delivery systems are on the order of days [7], i.e., 24 h. For simplicity, we set $\Delta t_i = T_{\text{Tx}}/I, \forall i \in \{1,\ldots,I\}$, and $N = 5$, and the value of the required absorption rate is

Parameter	Value	Parameter	Value
D_{X} [m²/s]	8×10^{-11}	D_{Rx} [m²/s]	0
a_{tx} [m]	1×10^{-7}	a_{rx} [m]	1×10^{-6}
T_{Tx} [h]	24	T_{Rx} [h]	24
r_0 [m]	10×10^{-6}	N	5
I	3000	$\theta(t)[\mathrm{s}^{-1}]$	1
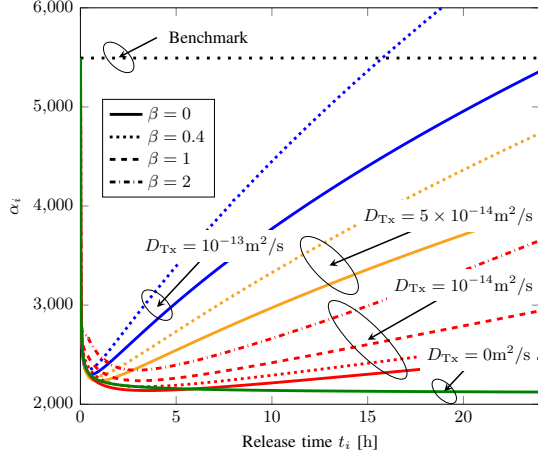
Fig. 2. Optimal release coefficients α_i as a function of release time t_i [h] for different system parameters. The black horizontal dotted line is the benchmark when the α_i are not optimized.

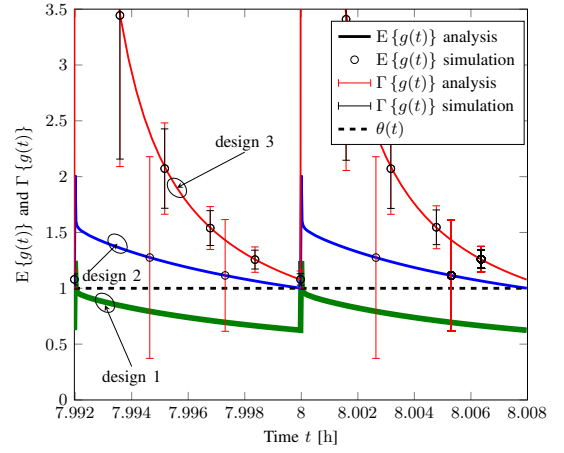Fig. 3. $\mathrm{E}\{g(t)\}$ and $\Gamma\{g(t)\}$ between the 1000-th release and the 1002-th release, i.e., at about 8 h, for three different designs. Design 1 (green line): naive design without considering Tx movement with $D_{\mathrm{Tx}} = 10^{-13}$ m²/s and $\beta = 0$; design 2 (blue line) and 3 (red line): optimal design with $\left(D_{\mathrm{Tx}}[\mathrm{m}^2/\mathrm{s}], \beta\right) = \left(10^{-13}, 0\right), \left(10^{-14}, 1\right)$, respectively.

set to $\theta(t) = 1\,\mathrm{s}^{-1}$. We choose I relatively large to obtain small intervals Δt_i. All simulation results are averaged over 10^5 independent realizations of the environment.

In Fig. 2, we plot the controlled-release coefficients α_i versus the corresponding release time t_i [h] for different system parameters. The coefficients are obtained by solving the optimization problem in (4) with $\beta = \{0, 0.4, 1, 2\}$ for $D_{\mathrm{Tx}} = 10^{-14}$ m²/s and $\beta = \{0, 0.4\}$ for $D_{\mathrm{Tx}} = \{5, 10\} \times 10^{-14}$ m²/s. As mentioned in the discussion of (3), we cannot choose large values of β when the diffusion coefficient is large, i.e., the standard deviation is large, as the problem may become infeasible. Fig. 2 shows that for all considered parameter settings, we should first release a large number of molecules for the absorption rate to exceed the threshold. Then, in the static system with $D_{\mathrm{Tx}} = 0\,\mathrm{m}^2/\mathrm{s}$, the optimal coefficient decreases with increasing time, since a fraction of the molecules previously released from the Tx linger around the Rx and are absorbed later. However, for the mobile time-variant channels, the Tx eventually diffuses away from the Rx as time t increases and hence, molecules released at later times by the Tx are far away from the Rx and may not reach the Rx. Therefore, at later times, the amount of drugs released has to be increased for the absorption rate to not fall below the threshold. For higher D_{Tx}, the Tx diffuses away from the Rx faster and thus, the coefficients α_i have to increase faster. This type of drug release is called a tri-phasic release [8]. Once we have designed the controlled-release profile, we can implement this by choosing a suitable drug carrier as shown in [8]. Moreover, as expected, with larger β, we need to release

more drugs to ensure that (4) is feasible. The black horizontal dotted line in Fig. 2 is a benchmark where the $\alpha_i, \forall i$, are not optimized but naively set to $\alpha_i = \alpha_1$. For this naive design, $A = \alpha_1 I \approx 1.65 \times 10^7$, whereas with the optimal α_i, for $\beta = 0$ and $D_{\mathrm{Tx}} = 10^{-13}$ [m²/s], $A = 1.2 \times 10^7$, i.e., equal to 73% of the naive design, and for $\beta = 1$ and $D_{\mathrm{Tx}} = 10^{-14}$ [m²/s], $A = 7.6 \times 10^6$, i.e., equal to 46% of the naive design. This highlights that applying the optimal controlled-release profile can save significant amounts of drugs and still satisfy the therapeutic requirements. Moreover, as observed in Fig. 2, the required values of α_i increase as t_i increases and thus the naive design with fixed α_i, i.e., the benchmark, cannot ultimately satisfy the required absorption rate.

In Fig. 3, we plot the mean and standard deviation of the absorption rate, $\mathrm{E}\{g(t)\}$ and $\Gamma\{g(t)\}$, between the 1000-th release and the 1002-th release for three designs, where we adopted $D_{\mathrm{Tx}} = 10^{-13}$ m²/s and $\beta = 0$ for designs 1 and 2, and $D_{\mathrm{Tx}} = 10^{-14}$ m²/s and $\beta = 1$ for design 3. Note that the considered time window, e.g., between the 1000-th release and the 1002-th release, is chosen arbitrarily in the middle of T_{Tx} to analyze the system behavior. For design 1, the Tx diffuses with $D_{\mathrm{Tx}} = 10^{-13}$ m²/s but the controlled release is designed without accounting for the Tx mobility, i.e., the adopted α_i are given by the green line in Fig. 2 obtained under the assumption of $D_{\mathrm{Tx}} = 0\,\mathrm{m}^2/\mathrm{s}$. For designs 2 and 3, the mobility of the Tx is taken into account. The black dashed line marks the threshold $\theta(t)$ that $g(t)$ should not fall below. It is observed from Fig. 3 that when the Tx diffuses but the design does not take into account the mobility, the requirement that the expected absorption rate, $\mathrm{E}\{g(t)\}$, exceeds $\theta(t)$, is not satisfied for most of the time. For design 2 with $\beta = 0$, we observe that $\mathrm{E}\{g(t)\} > \theta(t)$ always holds but $\mathrm{E}\{g(t)\} - \Gamma\{g(t)\} > \theta(t)$ does not always hold. For design 3 with $\beta = 1$, we observe that $\mathrm{E}\{g(t)\} - \Gamma\{g(t)\} > \theta(t)$ always holds since $\beta > 0$ enforces a gap between $\mathrm{E}\{g(t)\}$ and $\theta(t)$. In other words, even if $g(t)$ deviates from the mean, it can still exceed $\theta(t)$. Fig. 3 also shows that $\mathrm{E}\{g(t)\}$ first increases

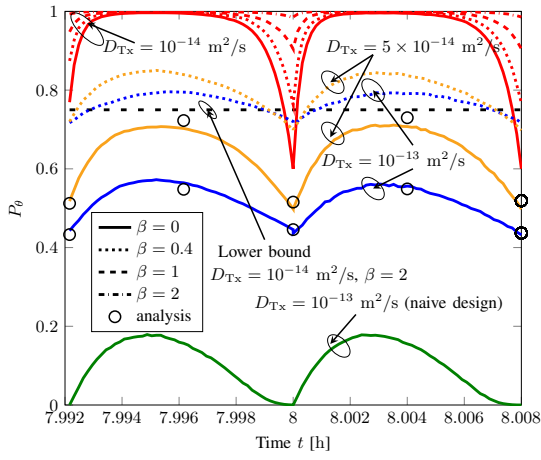Fig. 4. P_θ as a function of time t [h] between 1000-th release and 1002-th release, i.e., at about 8 h.

after a release and then decreases, due to the diffusion of the molecules. Furthermore, Fig. 3 confirms the accuracy of our derivations as the simulation results match the analytical results. Note that in the simulations, unlike the analysis, we have considered the reflection of the Tx when it hits the Rx. Therefore, the good agreement in Fig. 3 suggests that the reflection of the Tx does not have a significant impact on the numerical results and the approximation in (6) is valid.

In Fig. 4, we present the system performance in terms of P_θ, for the time period between the 1000-th and 1002-th releases, i.e., at about 8h. The lines and markers denote simulation and analytical results, respectively. Fig. 4 shows a good agreement between the analytical and simulation results. In Fig. 4, we observe that P_θ increases with increasing β because the design for larger β enforces a larger gap between $\mathrm{E}\{g(t)\}$ and $\theta(t)$, as can be seen in Fig. 3. Moreover, for a given β, P_θ will be different for different D_{Tx}. In particular, for larger D_{Tx}, P_θ is smaller due to the faster diffusion and less certainty about the CIR. Moreover, in Fig. 4, the green line shows that the naive design, i.e., design 1 in Fig. 3, has very poor performance. In Fig. 4, we also observe that between two releases, P_θ first increases due to the released drugs and then decreases due to drug diffusion. Furthermore, in Fig. 4, we show the lower bound on P_θ derived in Proposition 1 for $D_{\mathrm{Tx}} = 10^{-14}$ m^2/s and $\beta = 2$, where (17) yields $P_\theta \geqslant 0.75$. Fig. 4 shows that the red dash-dotted line, i.e., P_θ for $D_{\mathrm{Tx}} = 10^{-14}$ m^2/s and $\beta = 2$, is above the horizontal black dashed line, i.e., $P_\theta = 0.75$.

VI. CONCLUSIONS

In this paper, we considered a drug delivery system with a diffusive drug carrier and absorbing cells and modeled it as a time-variant channel between diffusive MC transceivers. We provided a statistical analysis of the time-variant CIR. Based on this statistical analysis, we designed the optimal controlled-release profile which minimizes the amount of released drugs while ensuring a targeted absorption rate of the drugs at the Rx for a prescribed time period. The probability of satisfying the constraint on the absorption rate was adopted as a system

performance criterion and was evaluated. We observed that ignoring the reality of Tx mobility in designing the release profile leads to unsatisfactory performance.

REFERENCES

[1] U. A. K. Chude-Okonkwo, R. Malekian, B. T. Maharaj, and A. V. Vasilakos, "Molecular communication and nanonetwork for targeted drug delivery: A survey," *IEEE Commun. Surveys Tuts.*, vol. 19, no. 4, pp. 3046–3096, May 2017.

[2] B. K. Lee, Y. H. Yun, and K. Park, "Smart nanoparticles for drug delivery: Boundaries and opportunities," *Chemical Engineering Science*, vol. 125, pp. 158–164, Apr 2015.

[3] K. B. Sutradhar and C. D. Sumi, "Implantable microchip: the futuristic controlled drug delivery system," *Drug Delivery*, vol. 23, no. 1, pp. 1–11, Apr 2014.

[4] M. Sefidgar, M. Soltani, K. Raahemifar, H. Bazmara, S. Nayinian, and M. Bazargan, "Effect of tumor shape, size, and tissue transport properties on drug delivery to solid tumors," *Journal of Biological Engineering*, vol. 8, no. 12, Jun 2014.

[5] A. Pluen, P. A. Netti, R. K. Jain, and D. A. Berk, "Diffusion of macromolecules in agarose gels: Comparison of linear and globular configurations," *Biophysical Journal*, vol. 77, no. 1, pp. 542–552, 1999.

[6] X. Wang, Y. Chen, L. Xue, N. Pothayee, R. Zhang, J. S. Riffle, T. M. Reineke, and L. A. Madsen, "Diffusion of drug delivery nanoparticles into biogels using time-resolved microMRI," *The Journal of Physical Chemistry Letters*, vol. 5, no. 21, pp. 3825–3830, Oct 2014.

[7] D. Y. Arifin, L. Y. Lee, and C. Wang, "Mathematical modeling and simulation of drug release from microspheres: Implications to drug delivery systems," *Advanced Drug Delivery Reviews*, vol. 58, no. 12, pp. 1274–1325, Sep 2006.

[8] S. Fredenberg, M. Wahlgren, M. Reslow, and A. Axelsson, "The mechanisms of drug release in poly(lactic-co-glycolic acid)-based drug delivery systems - A review," *International Journal of Pharmaceutics*, vol. 415, no. 1, pp. 34–52, May 2011.

[9] N. Farsad, H. B. Yilmaz, A. Eckford, C. B. Chae, and W. Guo, "A comprehensive survey of recent advancements in molecular communication," *IEEE Commun. Surveys Tuts.*, vol. 18, no. 3, pp. 1887–1919, Feb 2016.

[10] Y. Chahibi, M. Pierobon, and I. F. Akyildiz, "Pharmacokinetic modeling and biodistribution estimation through the molecular communication paradigm," *IEEE Trans. Biomed. Eng.*, vol. 62, no. 10, pp. 2410–2420, Oct 2015.

[11] M. Femminella, G. Reali, and A. V. Vasilakos, "A molecular communications model for drug delivery," *IEEE Trans. Nanobiosci.*, vol. 14, no. 8, pp. 935–945, Dec 2015.

[12] S. Salehi, N. S. Moayedian, S. S. Assaf, R. G. Cid-Fuentes, J. Sol-Pareta, and E. Alarcn, "Releasing rate optimization in a single and multiple transmitter local drug delivery system with limited resources," *Nano Commun. Netw.*, vol. 11, pp. 114–122, Mar 2017.

[13] S. Salehi, N. S. Moayedian, S. H. Javanmard, and E. Alarcn, "Life-time improvement of a multiple transmitter local drug delivery system based on diffusive molecular communication," *IEEE Trans. Nanobiosci.*, vol. 17, no. 3, pp. 352–360, Jul 2018.

[14] A. Ahmadzadeh, V. Jamali, and R. Schober, "Stochastic channel modeling for diffusive mobile molecular communication systems," *IEEE Trans. Commun.*, Jul. 2018, to be published.

[15] W. Haselmayr, S. M. H. Aejaz, A. T. Asyhari, A. Springer, and W. Guo, "Transposition errors in diffusion-based mobile molecular communication," *IEEE Commun. Lett.*, vol. 21, no. 9, pp. 1973–1976, Sep 2017.

[16] N. Varshney, W. Haselmayr, and W. Guo, "On flow-induced diffusive mobile molecular communication: First hitting time and performance analysis," [Online]. Available: https://arxiv.org/abs/1806.04784.

[17] H. B. Yilmaz, A. C. Heren, T. Tugcu, and C. Chae, "Three-dimensional channel characteristics for molecular communications with an absorbing receiver," *IEEE Commun. Lett.*, vol. 18, no. 6, pp. 929–932, June 2014.

[18] D. A. Stephens, "Mathematical statistics I," Lecture Notes, Fall 2008.

[19] G. H. Robertson, "Computation of the noncentral chi-square distribution," *The Bell System Technical Journal*, vol. 48, no. 1, pp. 201–207, Jan 1969.

[20] A. Papoulis and S. U. Pillai, *Probability, Random Variables and Stochastic Processes*. USA: McGraw-Hill, 2002.

[21] A. P. Prudnikov, Y. A. Brychkov, and O. I. Marichev, *Integrals and Series*. New York: Gordon and Breach Science, 1986, vol. 1.